Gutiérrez, I.; Garavís, M.; De Lorenzo, S.; Villasante, A.; González, C.; Arias-Gonzalez, JR. (2018). Single-Stranded Condensation Stochastically Blocks G-Quadruplex Assembly in Human Telomeric RNA. The Journal of Physical Chemistry Letters. 9(10):2498-2503. https://doi.org/10.1021/acs.jpclett.8b00722

Single-stranded Condensation Stochastically Blocks G-quadruplex Assembly in Human Telomeric RNA

*Irene Gutiérrez[1], Miguel Garavís[2], Sara de Lorenzo[1], Alfredo Villasante[3], Carlos González[2], and J. Ricardo Arias-Gonzalez[1,4]**

[1]Instituto Madrileño de Estudios Avanzados en Nanociencia (IMDEA Nanociencia). Cantoblanco, 28049 Madrid, Spain

[2]Instituto de Química Física Rocasolano, CSIC, C/Serrano 119, 28006 Madrid, Spain

[3]Centro de Biología Molecular "Severo Ochoa" CSIC-UAM, C/Nicolás Cabrera 1, 28049 Madrid, Spain

[4]CNB-CSIC-IMDEA Nanociencia Associated Unit "Unidad de Nanobiotecnología"

TERRA is an RNA molecule transcribed from human subtelomeric regions towards chromosome ends potentially involved in regulation of heterochromatin stability, semiconservative replication and telomerase inhibition, among others. TERRA contains tandem repeats of the sequence GGGUUA, with a strong tendency to fold into a four-stranded arrangement known as parallel G-quadruplex. Here, we demonstrate by using single-molecule force spectroscopy that this potential is limited by the inherent capacity of RNA to self-associate randomly and further condense into entropically more favorable structures. We stretched RNA constructions with more than four and less than eight hexanucleotide repeats, thus unable to form several G-quadruplexes in tandem, flanked by non-G-rich overhangs of random sequence by optical tweezers on a one by one basis. We found that condensed RNA stochastically blocks G-quadruplex folding pathways with a near 20% probability, a behavior that is not found in DNA analogous molecules.

TOC GRAPHICS

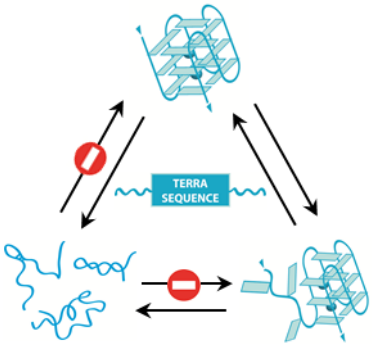

KEYWORDS. TERRA, G-quadruplex, RNA, DNA, optical tweezers, single-molecule, folding.

The G-quadruplex is a four-stranded nucleic acid structure formed by G-rich sequences[1]. G-quadruplexes are preferentially formed in some genome regions, such as telomeres, gene promoters (including oncogene promoters) and ribosomal DNA (rDNA)[2-4]. G-quadruplexes can also form at RNA level and are particularly frequent in untranslated mRNA regions[5-6]. It is nowadays accepted that G-quadruplexes exist in vivo[7] and play important roles in multiple key biological processes, such as transcription, replication, translation, and telomere maintenance[3-7]. Recently, it has been found that telomeres are transcribed into TElomeric Repeat containing RNA (TERRA), which holds several repetitions of the sequence GGGUUA at their 3' end[8-11]. TERRA is thus capable of forming G-quadruplex structures in vitro and has the potential to do so in vivo[12-13]. TERRA is a non-coding RNA proposed to act as a scaffold for the assembly of telomeric proteins involved in telomere maintenance and telomeric heterochromatin formation[10, 13-19].

G-quadruplex folding/unfolding processes have been studied by a number of theoretical [20-24] and experimental methods, including spectroscopic-based techniques[21, 25], mass spectrometry[26] and NMR[27]. However, most of the experimental methods do not represent the dynamical scenarios in which localized forces are applied by specialized proteins, such as the telomerase, to a single molecular structure in the cell. Here, we report on the unfolding dynamics of short TERRA molecules in the presence of extra single-stranded (ss) RNA. We singled out several repetitions, n, of the human telomeric sequence GGGUUA and added extra nucleotides (nts) of non-G-rich, random sequences on both the 3' and 5' ends of ssRNA (see Figure 1(A), Figure S1 and the experimental section in the Supporting Information document). We chose $4 < n < 8$, first, to make sure that the sequence can only fold into a single G-quadruplex conformation and, second, to study the effect of additional repetitions in the formation of this non-canonical structure.

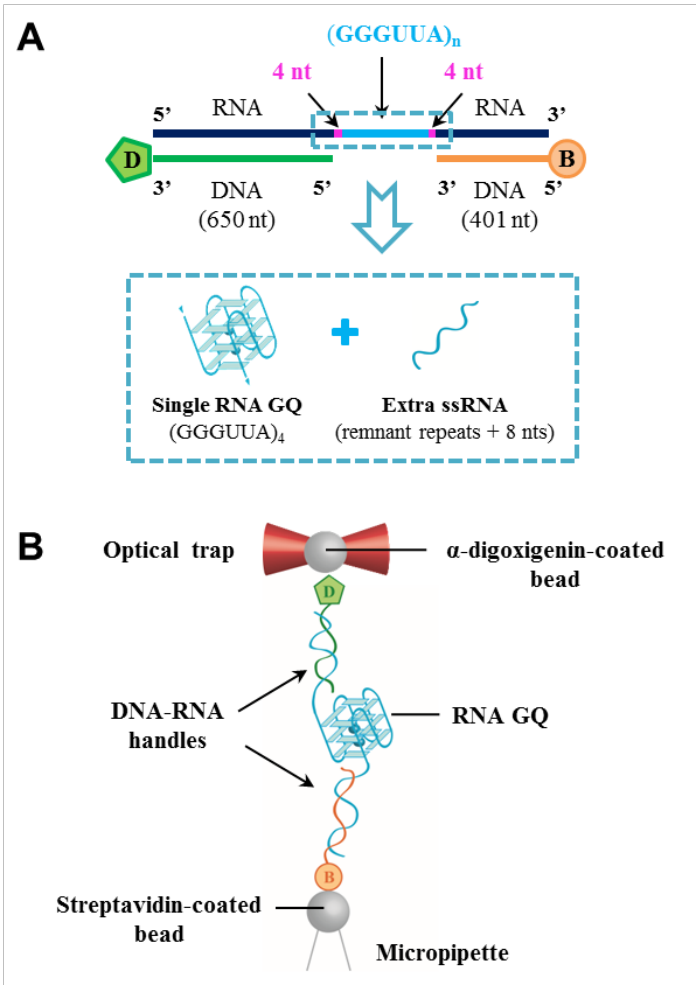

Figure 1. Scheme of the experimental configuration. (A) Molecular construction. It consists of a central sequence with "n" repeats of GGGUUA, which may yield a single RNA G-quadruplex (GQ, represented) or a randomly condensed ssRNA (see text for details). (B) Experimental set-up: a single RNA construct was tethered by opposite hybrid duplex ends between two polystyrene microspheres: an α-digoxigenin-coated bead, optically trapped, and a streptavidin-coated bead, held by air suction on top of a micropipette. "B" stands for biotin and "D" for digoxigenin.

For reference purposes, we will focus on the five-repeat molecule (n = 5) with four extra nucleotides on both the 3' and 5' ends. These spacer tracts were added to provide elasticity to the central key sequence, following the double-stranded handles, which are mechanically more rigid

to bending. Within RNA preparation restraints, spacers sequences were selected to minimize any possible interference with the G-quadruplex formation. Earlier experiments therein by circular dichroism and NMR with this RNA fragment demonstrated its potential to form an intramolecular parallel G-quadruplex[28]. We will next show that the 8-nt ssRNA excess together with an extra GGGUUA repetition provides enough configurational flexibility for this telomeric sequence to fold into several conformations (see Results and Discussion section and Figure S2 in the Supporting Information document). This 38-nt sequence can give rise to: (i) a four-stranded, G-quadruplex structure interacting with different lengths of excess ssRNA on both ends (see Figure S2), (ii) a three-stranded, G-triplex similarly coexisting with two ssRNA lateral fragments of variable lengths and (iii) either a hairpin-like structure or more general condensed conformations of ssRNA. These structural and subsequent kinetic scenarios as well as the probabilities for the conformations discussed above resemble the complex picture described for G-quadruplex DNA folding[23, 29]. Real-time single-molecule techniques are very well-suited to unveil the intricate dynamics inherent to G-quadruplex folding/unfolding, since bulk approaches in which an ensemble of equal preparations takes place can only provide average signals thus hindering the access to the less populated conformations[30-31].

We used optical tweezers (OT) to study single-molecule mechanical folding and unfolding processes under controlled in vitro conditions. To this end, the 38-nt reference ssRNA sequence was attached to polystyrene beads, as shown in Figure 1(B), through hybrid DNA-RNA handles. Rupture events became observable as jumps over the characteristic force-extension curves of the double-stranded (ds) hybrid handles, whose elastic response is similar to those of dsDNA and dsRNA[32-33]. We registered two categories of behaviors: (i) curves with single rupture events and (ii) those with two consecutive ones, which we analyze next.

Single rupture events. Force-extension curves with only one rupture event represented the typical behavior. Figure S3 shows the results of several single molecules with the reference sequence. The traces mostly reveal the characteristic elasticity of the double-stranded handles

interrupted by rupture events at intermediate forces. Some of the traces revealed the overstretching transition of the hybrid handles, this fact confirming that only one molecular construct has been attached between the beads[32]. Rupture signatures correspond to unfolding events of different species, as judged by their force and extension values and also by the relaxation behavior of the traces (see also the insets).

Three different types of rupture events can be distinguished and they can be assigned, a priori, to the unfolding of different structures by estimating the released ssRNA. Let L_{nt} be the mean, effective distance between successive nucleotides in ssRNA, d_G the solution-structure distance between first and last nucleotides in the G-structure (PDB ID: 2KBP)[34-35], N_G the number of nucleotides in the folded G-structure and x the rupture extension measured in the OT experiments, then: $x = N_G \times L_{nt} - d_G$. The estimated released extension upon the G-quadruplex and the G-triplex ruptures are: 21 (nt) × L_{nt} – 1.5 (nm) = 9.2 nm and 15 (nt) × L_{nt} – 1.9 (nm) = 5.8 nm, respectively, where we have used L_{nt} = 0.51 nm/nt following Yangyuoru et al.[35] (see also the Supplementary Discussion in the Supporting Information document). We conclude that the most probable rupture events arise from the unfolding of the G-quadruplex/G-triplex, Figure S3(A), and a more general structure that may take place as a consequence of the ssRNA non-specific self-interactions, Figure S3(B). This interpretation agrees with previous studies, where the G-triplex and G-quadruplex rupture events were located primarily in the range of 20-30 pN[35]. The interpretation of the rupture event at low force is related to the decondensation plateau in the force-extension curves of plain single-stranded nucleic acids, between 4-10 pN, depending on ionic conditions[36-39] (see Supplementary Discussion).

To in situ confirm this probabilistic association we recorded data over almost 300 rupture events of this reference molecular construct. The statistical analysis of the force-extension curves for single-rupture events is presented in Figure 2 in parallel with DNA analogous molecules with the same sequence (see Figure S4 for unfolding-refolding curves of the DNA G-quadruplex sequence). Figure 2(A), left panel, shows the statistical behavior of the rupture forces for RNA.

Two major populations can be distinguished centered at nearly 9 and 22 pN. The structures that we propose as majorly responsible for the two populations are condensed ssRNA (due to ssRNA non-specific self-interactions, see also the Supplementary Discussion) for the lower and narrower force peak and the G-quadruplex/G-triplex unfolding for the higher and wider force peak (Supplementary Discussion). Figure 2(A), right panel, shows the unfolding extension histogram.

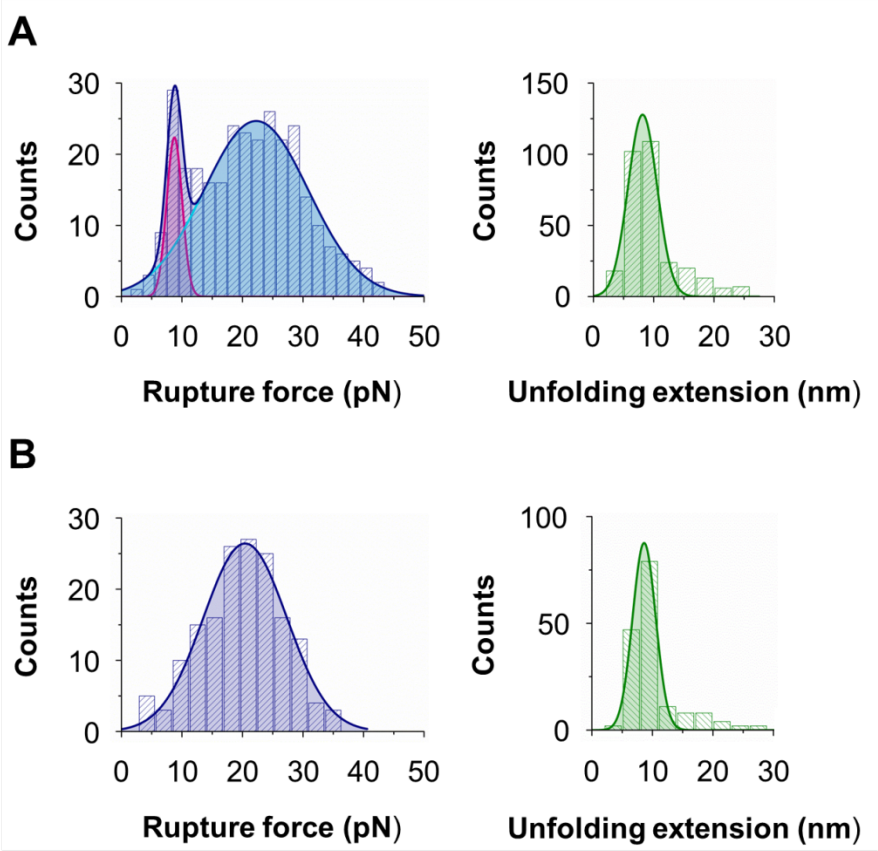

Figure 2. Statistics of single rupture events in the reference sequence. Rupture force and unfolding extension distribution for (A) the RNA construction of 5 repeats (N=299) and (B) its analogue in DNA (N= 163). Mean ± standard error (s.e.) and standard deviation (s.d.) according to Gaussian fitting are: (A) 8.8 ± 0.2 and 1.3 pN (pink line), 22.3 ± 0.5 and 8.6 pN (light blue line), left panel, 8.2 ± 0.2 and 2.4 nm (green line), right panel; and (B) 20.4 ± 0.4 and 6.9 pN (blue line, left panel), 8.6 ± 0.1 and 1.9 nm (green line, right panel). In the left panel of (A), dark blue line corresponds to a Gaussian double-peak fit.

Figure 2(B) shows the statistics of unfolding/refolding experiments with an equivalent molecular construct entirely made of DNA, thus preserving the sequence of both the central single-stranded segment and the double-stranded handles for attachment to beads. This molecule has also a potential to fold into a G-quadruplex, as reflected in the force-extension curves of Figure S4. Its rupture force statistics, Figure 2(B), left panel, exhibits a single broad peak center at around the same force of that corresponding to the G-quadruplex/G-triplex. The peak force is shifted to the left by less than 2 pN with respect to the RNA distribution corresponding to the G-quadruplex/G-triplex, in agreement with previous works that reported that DNA G-quadruplex unfold at lower force[40-44]. The most important feature of these control experiments is the absence of a peak near 9 pN, which indicates that the potential of the RNA molecule to self-fold non-specifically and thus block highly organized non-canonical structures is unique. The experiments with this DNA analogue were measured in a high-resolution instrument (see the experimental section in the Supporting Information document and Figure S4) to confirm the low probability of rupture events at low forces.

To further confirm the interpretation of the two statistical populations for TERRA, two filters in extension were applied to the histogram in Figure 2 (A), left panel, based on the theoretical dimensions of G-triplex and G-quadruplex structures[35]: a low-pass filter with a cutoff extension of 12 nm, which favors rupture events corresponding to the unfolding of the G-quadruplex/G-triplex conformations and a high-pass filter above 12 nm, which favors the populations corresponding to the unfolding of hairpins and those with more random behavior related with ssRNA non-specific self-interactions[45-47]. Figure 3 shows the resulting force histograms. The populations correlate with the expected conformations. Namely, Figure 3(A) shows a broad peak centered at approximately the same force as that shown for the wide population in Figure 2(A), left panel, and that has been attributed to the G-quadruplex/G-triplex, and the histogram in Figure 3(B) populates majorly the low forces, including a peak at 7-9 pN similar to the narrow one in Figure 2(A), left panel, which has been associated to generally condensed ssRNA structures.

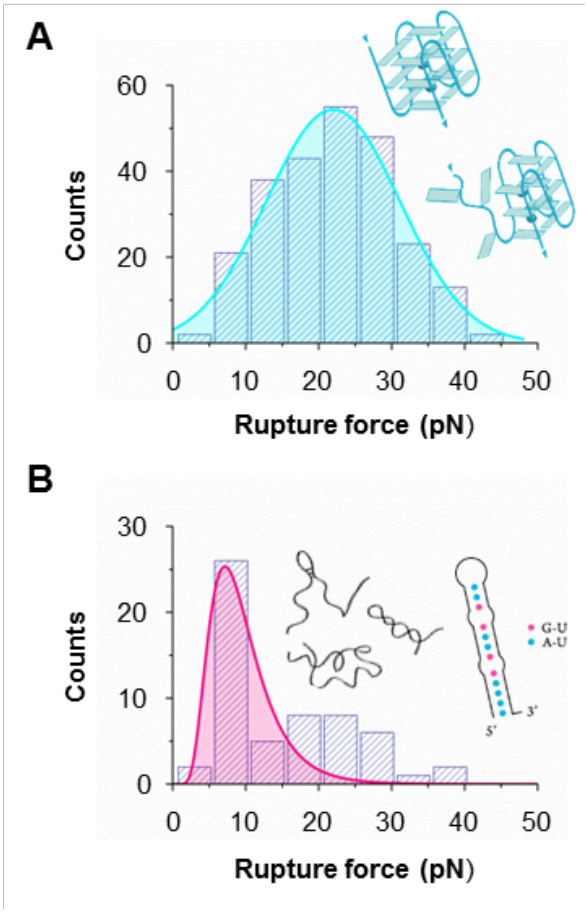

Figure 3. Rupture force distributions for the different conformations in the reference sequence. (A) G-quadruplex and G-triplex (N= 241, 80.6%), data filtered in the range [0, 12] nm. Mean ± s.e. and s.d. according to Gaussian fitting are 22.0 ± 0.6 and 9.3 pN. (B) Duplex or other condensed conformations (N=58, 19.4%), data filtered in the range (12, 26] nm. Median ± s.d. according to a log-normal distribution is 8.7 ± 4.4 pN. Peak value (mode) ± s.e. is 7.2 ± 1.2 pN.

To study the behavior of the stochastic blockage with the number of repeats and with flanking sequences different from the previously analyzed one, we synthetized three other molecular constructs: a 6-repeat and a 7-repeat molecules flanked by the same random sequences as previously used (44 and 50 nts, respectively) and a 5-repeat construction with more extra random RNA sequence (44 nts) (see the experimental section in the Supporting Information document). The qualitative behavior is maintained for single rupture events, as reflected in their force-

extension curves (Figures S5-S7): rupture events at both high forces, compatible with G-quadruplex/G-triplex, and low forces, related to condensation, are observed. Bimodal rupture force distributions (Figures S8 and S9) confirm the stochastic effect, which probability increases with the number of repeats and decreases with length of the extra random sequence. These trends correlate with the number of Gs, a very promiscuous nucleobase thus tending to increase the probability of a condensate in RNA.

Consecutive rupture events. The category of force-extension curves with two consecutive rupture events was significantly less probable, as we analyzed next. Figures S10-S13 show characteristic force-extension curves corresponding to different molecules with sequential rupture events for the TERRA molecules with 5-7 repeats and extra random sequence. As discussed above, the formation of condensed ssRNA blocks the assembly of the G-triplex and the G-quadruplex. Nevertheless, when one of these non-canonical structures assembles, it may interact with the excess ssRNA in the sequence. Then, the mechanical unfolding should provoke the separation of the extra ssRNA from the G-quadruplex or G-triplex before the full opening of the structure. According to the forces and extensions found in Figure S10-S13, this is the most probable scenario for the analyzed molecules. The statistical analysis of the 5-repeat TERRA molecule, Figure 4, confirms this interpretation when two consecutive rupture events are observed in the force-extension curves: the first rupture peak complies with low forces and short extensions, Figure 4(A), and the second one with high forces and typical extensions for the G-quadruplex and G-triplex, Figure 4(B). The statistics corresponding to the 6 and 7-repeat TERRA molecules and to those with 5 repeats and extra random sequence, Figure S14, confirm this trend. Peak forces and peak extensions are compatible with the single-rupture event statistics, both for the ssRNA condensates and the G-quadruplex, thus supporting this interpretation.

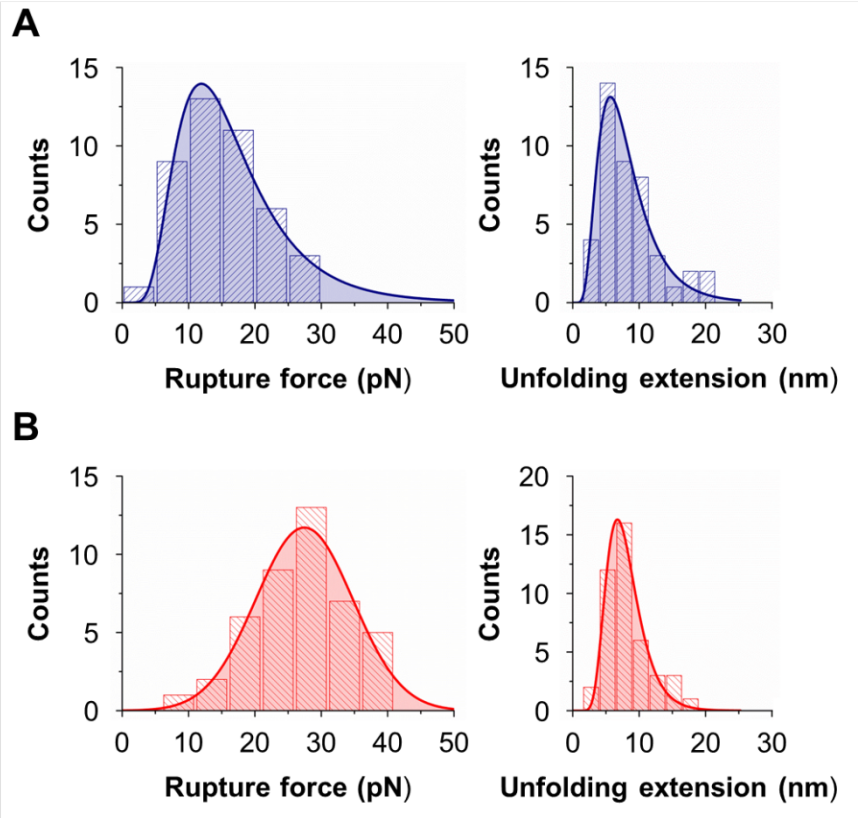

Figure 4. Statistics of single-molecule sequential unfolding events in the reference sequence (N=43). (A) Rupture force and unfolding extension distributions for the first rupture event. Median and s.d. according to a log-normal fitting for this force distribution are 14.9 and 8.3 pN (peak value (mode) ± s.e., 11.9 ± 0.5 pN). Median and s.d. for the unfolding extension distribution are 7.3 and 4.4 nm (peak value (mode) ± s.e., 5.7 ± 0.4 nm). (B) Rupture force and unfolding extension distributions for the second rupture event. Mean ± s.e. and s.d. for this force distribution, according to a Gaussian fitting (red line) are 27.4 ± 0.5 and 7.3 pN. Median and s.d. according to log-normal fitting for the unfolding extension distribution are 7.6 and 2.8 nm (peak value (mode) ± s.e., 6.7 ± 0.2 nm).

Importantly, it is observed that the probability of interaction of the formed G-quadruplex with the single-stranded RNA excess increases with the number of added nucleotides: 12.6%, 17.4% and 26.1% for 5, 6 and 7 repeats, and 27% for the 5-repeat molecule with more extra random

ssRNA. This trend was expected for longer molecules since self-interactions allowed by the bending elasticity are more probable.

The probability of formation of a non-canonical structure can be calculated based on the next heuristic inference:

$$P(\text{G-QT}) = P(\text{consecutive RE}) + P(\text{single RE}) \times P(\text{G-QT}|\text{single RE}) \quad (1)$$

where G-QT stands for G-quadruplex or G-triplex, RE stands for rupture event and the vertical bar denotes conditional probability. The results, along with the previously presented experimental probabilities, are shown on Table S1. It is observed that the number of repeats hardly affects the probability of formation of the G-quadruplex/G-triplex, slightly above an 80%, and that the addition of random nucleotides flanking the hexanucleotide repeats attenuates the stochastic blockage raising the probability of the non-canonical structure formation to a 90%.

Single rupture events as those represented in Figures S3-S7 may correspond to separate events sequential but proximal in force, which would match to the release of one arm of the G-quadruplex rapidly followed by the rupture of the G-triplex into ssRNA. Neither these events nor the G-hairpin unfolding[48-50] could be distinguished within our experimental resolution. Although some force-extension curves with two rupture events in our experiments could be interpreted in this fashion, we have not found sufficient statistical significance. Then, we conclude that, if in-pathway, G-triplex and G-hairpin breakage takes place almost simultaneously after the G-quadruplex disassembly in our experiments; that is, the sequential release of the GGGUUA arms of the G-quadruplex are detected within the same rupture event in the force-extension curves at the herein used experimental velocity.[44] A triangular, three state kinetic model, as that proposed elsewhere[35,51-53], is compatible with our results (see the abstract figure).

The dynamic behavior of the rupture events has another feature in the stretch-relaxation cycles: the reversibility. Refolding during relaxation is the normal behavior but the mechanical hysteresis is typically lower for the duplexes with respect to the G-quadruplex or G-triplex

conformations, as measured by the degree of overlapping of the stretch and relaxation traces (see Figures S3-S7). The refolding is more likely for the duplex than for the G-triplex or G-quadruplex since these latter conformations involve the ordered assembly of three and four strands, respectively, within similar time frames, which is less probable than the assembly of randomly-condensed ssRNA or duplexes, with lower entropy. Then, it is expected that the non-canonical conformations involve refolding further from equilibrium than simpler conformations at the same loading rate.

Free energies can be recovered by using Jarzynski's equality, which evaluates this equilibrium thermodynamic potential increment from non-equilibrium work measurements (see Supporting Information document)[54]. Tables S2 and S3 collect the work calculated from our experiments for the non-canonical structure and the condensates, respectively, in each molecular preparation. Tables S4 and S5 show the corresponding Gibbs free energy results. For the 5-repeat DNA analogous molecule, we obtained $\Delta G = -(6.9 \pm 0.6)$ kcal/mol, which is similar within experimental error to earlier bulk reports that yielded −7.1 kcal/mol for the parallel G-quadruplex assembled with a four-repeat molecule[55]. This consistency serves as a control check, both from a qualitative and a quantitative viewpoint, for our results at the single-molecule level. RNA G-quadruplex has always higher Gibbs free energy increment (in absolute value) than the DNA analogue, also consistent with earlier literature[35].

Although condensed ssRNA conformations have lower stability per nucleotide (see Tables S2-S5) than the G-triplex or the G-quadruplex, the overall energy is higher for the former. Therefore, folding pathways that give rise to condensates, with distinct hydration and which are entropically favored, cannot be discarded in a cellular context. The formation of a condensed ssRNA knot instead of a G-quadruplex/G-triplex can largely facilitate its denaturation by specialized protein machinery; specifically, decondensing the ssRNA involves an average force barrier near 10 pN, whereas that of the G-triplex or the G-quadruplex is on average above 20 pN.

In conclusion, we have found a remarkable conformational competition between unspecific self-interacting ssRNA species and the G-quadruplex or the G-triplex conformations. This phenomenon, which only occurs in RNA and not in DNA species, is due to the G-rich nature of the sequence. Although expected for random ribonucleic sequences, this behavior has neither been observed nor quantified for this genomically central RNA tract. Furthermore, to our knowledge, this is the first demonstration of a conformational stochastic blockage in a biological nanostructure, which we show in an important molecule. Although any G-rich RNA sequence may produce strong condensation, the G-quadruplex forming sequences are inherently G-rich, thus concomitantly generating the reported stochastic blockage. Considering that the structural state of TERRA tracts determines its function, we believe that the condensed ssRNA stochastic blockage may show relevant to understand TERRA regulation in telomeric heterochromatin stability or in telomerase inhibition, apart from being an important knowledge to counteract TERRA function by drug-targeting in tumorigenesis and senescence.

ASSOCIATED CONTENT

Supporting Information. Detailed process of synthesis, replicates of force-extension curves and additional statistics and notes. This material is available free of charge.

AUTHOR INFORMATION

Corresponding author

*ricardo.arias@imdea.org

Notes

The authors declare no competing financial interests.

ACKNOWLEDGMENT

Dedicated to the memory of Alfredo Villasante.

The authors thank E. Poyatos-Racionero for auxiliary experiments. I.G. is supported by Fundación IMDEA Nanociencia and M.G. by an FPI fellowship (BES-2009-027909). This research has received grants from the MINECO (MAT2015-71806-R and BFU2017-89707-P). IMDEA Nanociencia acknowledges support from the 'Severo Ochoa' Programme for Centres of Excellence in R&D (MINECO, Grant SEV-2016-0686).

REFERENCES

1. Sen, D.; Gilbert, W. Formation of Parallel Four-Stranded Complexes by Guanine-Rich Motifs in DNA and Its Implications for Meiosis. *Nature* **1988**, *334*, 364.
2. Chambers, V. S.; Marsico, G.; Boutell, J. M.; Di Antonio, M.; Smith, G. P.; Balasubramanian, S. High-Throughput Sequencing of DNA G-Quadruplex Structures in the Human Genome. *Nat. Biotechnol.* **2015**, *33*, 877.
3. Rhodes, D.; Lipps, H. J. G-Quadruplexes and Their Regulatory Roles in Biology. *Nucleic Acids Res.* **2015**, *43*, 8627-8637.
4. Hänsel-Hertsch, R.; Di Antonio, M.; Balasubramanian, S. DNA G-Quadruplexes in the Human Genome: Detection, Functions and Therapeutic Potential. *Nat. Rev. Mol. Cell. Biol.* **2017**, *18*, 279.
5. Kumari, S.; Bugaut, A.; Huppert, J. L.; Balasubramanian, S. An RNA G-Quadruplex in the 5□ UTR of the NRAS Proto-Oncogene Modulates Translation. *Nat. Chem. Biol.* **2007**, *3*, 218-221.
6. Bugaut, A.; Balasubramanian, S. 5□-UTR RNA G-Quadruplexes: Translation Regulation and Targeting. *Nucleic Acids Res.* **2012**, *40*, 4727-4741.
7. Biffi, G.; Tannahill, D.; McCafferty, J.; Balasubramanian, S. Quantitative Visualization of DNA G-Quadruplex Structures in Human Cells. *Nat. Chem.* **2013**, *5*, 182.
8. Azzalin, C. M.; Reichenbach, P.; Khoriauli, L.; Giulotto, E.; Lingner, J. Telomeric Repeat Containing RNA and RNA Surveillance Factors at Mammalian Chromosome Ends. *Science* **2007**, *318*, 798-801.
9. Schoeftner, S.; Blasco, M. A. Developmentally Regulated Transcription of Mammalian Telomeres by DNA-Dependent RNA Polymerase II. *Nat. Cell Biol.* **2008**, *10*, 228-36.
10. Feuerhahn, S.; Iglesias, N.; Panza, A.; Porro, A.; Lingner, J. TERRA Biogenesis, Turnover and Implications for Function. *FEBS Lett.* **2010**, *584*, 3812-8.

11. Porro, A.; Feuerhahn, S.; Reichenbach, P.; Lingner, J. Molecular Dissection of Telomeric Repeat-Containing RNA Biogenesis Unveils the Presence of Distinct and Multiple Regulatory Pathways. *Mol. Cell. Biol.* **2010**, *30*, 4808-17.
12. Xu, Y.; Suzuki, Y.; Ito, K.; Komiyama, M. Telomeric Repeat-Containing RNA Structure in Living Cells. *Proc. Natl. Acad. Sci. U. S. A.* **2010**, *107*, 14579-84.
13. Biffi, G.; Tannahill, D.; Balasubramanian, S. An Intramolecular G-Quadruplex Structure Is Required for Binding of Telomeric Repeat-Containing RNA to the Telomeric Protein TRF2. *J. Am. Chem. Soc.* **2012**, *134*, 11974-11976.
14. Horard, B.; Gilson, E. Telomeric RNA Enters the Game. *Nat. Cell Biol.* **2008**, *10*, 113-114.
15. Deng, Z.; Norseen, J.; Wiedmer, A.; Riethman, H.; Lieberman, P. M. TERRA RNA Binding to TRF2 Facilitates Heterochromatin Formation and ORC Recruitment at Telomeres. *Mol. Cell* **2009**, *35*, 403-13.
16. Luke, B.; Lingner, J. TERRA: Telomeric Repeat-Containing RNA. *EMBO J.* **2009**, *28*, 2503-2510.
17. Lopez de Silanes, I.; Stagno d'Alcontres, M.; Blasco, M. A. TERRA Transcripts Are Bound by a Complex Array of RNA-Binding Proteins. *Nat. Commun.* **2010**, *1*, 33.
18. Redon, S.; Reichenbach, P.; Lingner, J. The Non-Coding RNA TERRA Is a Natural Ligand and Direct Inhibitor of Human Telomerase. *Nucleic Acids Res.* **2010**, *38*, 5797-5806.
19. Lopez de Silanes, I.; Grana, O.; De Bonis, M. L.; Dominguez, O.; Pisano, D. G.; Blasco, M. A. Identification of TERRA Locus Unveils a Telomere Protection Role Through Association to Nearly All Chromosomes. *Nat. Commun.* **2014**, *5*, 4723.
20. Yang, C.; Kulkarni, M.; Lim, M.; Pak, Y. In Silico Direct Folding of Thrombin-Binding Aptamer G-Quadruplex at All-Atom Level. *Nucleic Acids Res.* **2017**, *45*, 12648-12656.
21. Aznauryan, M.; Søndergaard, S.; Noer, S. L.; Schiøtt, B.; Birkedal, V. A Direct View of the Complex Multi-Pathway Folding of Telomeric G-Quadruplexes. *Nucleic Acids Res.* **2016**, gkw1010.
22. Stadlbauer, P.; Trantírek, L.; Cheatham III, T. E.; Koča, J.; Šponer, J. Triplex Intermediates in Folding of Human Telomeric Quadruplexes Probed by Microsecond-Scale Molecular Dynamics Simulations. *Biochimie* **2014**, *105*, 22-35.
23. Šponer, J.; Bussi, G.; Stadlbauer, P.; Kührová, P.; Banáš, P.; Islam, B.; Haider, S.; Neidle, S.; Otyepka, M. Folding of Guanine Quadruplex Molecules–Funnel-Like Mechanism or Kinetic Partitioning? An Overview from MD Simulation Studies. *Biochim. Biophys. Acta* **2017**, *1861*, 1246-1263.

24. Limongelli, V.; De Tito, S.; Cerofolini, L.; Fragai, M.; Pagano, B.; Trotta, R.; Cosconati, S.; Marinelli, L.; Novellino, E.; Bertini, I. The G-Triplex. *Angew. Chem. Int. Ed* **2013**, *125*, 2325-2329.

25. Lee, J.; Okumus, B.; Kim, D.; Ha, T. Extreme Conformational Diversity in Human Telomeric DNA. *Proc. Natl. Acad. Sci. U.S.A.* **2005**, *102*, 18938-18943.

26. Marchand, A.; Gabelica, V. Folding and Misfolding Pathways of G-Quadruplex DNA. *Nucleic Acids Res.* **2016**, gkw970.

27. Bessi, I.; Jonker, H. R.; Richter, C.; Schwalbe, H. Involvement of Long□Lived Intermediate States in the Complex Folding Pathway of the Human Telomeric G□Quadruplex. *Angew. Chem. Int. Ed.* **2015**, *54*, 8444-8448.

28. Garavís, M.; Bocanegra, R.; Herrero-Galán, E.; González, C.; Villasante, A.; Arias-Gonzalez, J. R. Mechanical Unfolding of Long Human Telomeric RNA (TERRA). *Chem. Commun.* **2013**, *49*, 6397-6399.

29. Gabelica, V. A Pilgrim's Guide to G-Quadruplex Nucleic Acid Folding. *Biochimie* **2014**, *105*, 1-3.

30. Hormeno, S.; Arias-Gonzalez, J. R. Exploring Mechanochemical Processes in the Cell with Optical Tweezers. *Biol. Cell* **2006**, *98*, 679-95.

31. Bustamante, C. In Singulo Biochemistry: When Less Is More. *Annu. Rev. Biochem.* **2008**, *77*, 45-50.

32. Herrero-Galan, E.; Fuentes-Perez, M. E.; Carrasco, C.; Valpuesta, J. M.; Carrascosa, J. L.; Moreno-Herrero, F.; Arias-Gonzalez, J. R. Mechanical Identities of RNA and DNA Double Helices Unveiled at the Single-Molecule Level. *J. Am. Chem. Soc.* **2013**, *135*, 122-31.

33. Arias-Gonzalez, J. R. Single-Molecule Portrait of DNA and RNA Double Helices. *Integr Biol (Camb)* **2014**, *6*, 904-25.

34. Martadinata, H.; Phan, A. T. Structure of Propeller-Type Parallel-Stranded RNA G-Quadruplexes, Formed by Human Telomeric RNA Sequences in K^+ solution. *J. Am. Chem. Soc.* **2009**, *131*, 2570-8.

35. Yangyuoru, P. M.; Zhang, A. Y.; Shi, Z.; Koirala, D.; Balasubramanian, S.; Mao, H. Mechanochemical Properties of Individual Human Telomeric RNA (TERRA) G-Quadruplexes. *ChemBioChem* **2013**, *14*, 1931-5.

36. Bizarro, C. V.; Alemany, A.; Ritort, F. Non-Specific Binding of Na^+ and Mg^{2+} to Rna Determined by Force Spectroscopy Methods. *Nucleic Acids Res.* **2012**, *40*, 6922-35.

37. Alemany, A.; Ritort, F. Determination of the Elastic Properties of Short ssDNA Molecules by Mechanically Folding and Unfolding DNA Hairpins. *Biopolymers* **2014**, *101*, 1193-9.

38. Bosco, A.; Camunas-Soler, J.; Ritort, F. Elastic Properties and Secondary Structure Formation of Single-Stranded DNA at Monovalent and Divalent Salt Conditions. *Nucleic Acids Res.* **2014**, *42*, 2064-74.
39. de Lorenzo, S.; Ribezzi-Crivellari, M.; Arias-Gonzalez, J. R.; Smith, S. B.; Ritort, F. A Temperature-Jump Optical Trap for Single-Molecule Manipulation. *Biophys. J.* **2015**, *108*, 2854-64.
40. Yu, Z.; Schonhoft, J. D.; Dhakal, S.; Bajracharya, R.; Hegde, R.; Basu, S.; Mao, H. ILPR G-Quadruplexes Formed In Seconds Demonstrate High Mechanical Stabilities. *J. Am. Chem. Soc.* **2009**, *131*, 1876-82.
41. de Messieres, M.; Chang, J. C.; Brawn-Cinani, B.; La Porta, A. Single-Molecule Study of G-Quadruplex Disruption Using Dynamic Force Spectroscopy. *Phys. Rev. Lett.* **2012**, *109*, 058101.
42. Lorenz, R.; Bernhart, S. H.; Qin, J.; Honer zu Siederdissen, C.; Tanzer, A.; Amman, F.; Hofacker, I. L.; Stadler, P. F. 2D Meets 4G: G-Quadruplexes in RNA Secondary Structure Prediction. *IEEE/ACM Trans. Comput. Biol. Bioinform.* **2013**, *10*, 832-44.
43. Yu, Z.; Mao, H. Non-B DNA Structures Show Diverse Conformations and Complex Transition Kinetics Comparable to RNA or Proteins-a Perspective from Mechanical Unfolding and Refolding Experiments. *Chem. Rec.* **2013**, *13*, 102-16.
44. Bergues-Pupo, A. E.; Arias-Gonzalez, J. R.; Moron, M. C.; Fiasconaro, A.; Falo, F. Role of the Central Cations in the Mechanical Unfolding of DNA and RNA G-Quadruplexes. *Nucleic Acids Res.* **2015**, *43*, 7638-47.
45. Hardin, C. C.; Watson, T.; Corregan, M.; Bailey, C. Cation-Dependent Transition Between the Quadruplex and Watson-Crick Hairpin Forms of d(CGCG$_3$GCG). *Biochemistry* **1992**, *31*, 833-41.
46. Bugaut, A.; Murat, P.; Balasubramanian, S. An RNA Hairpin to G-Quadruplex Conformational Transition. *J. Am. Chem. Soc.* **2012**, *134*, 19953-6.
47. Kuo, M. H.; Wang, Z. F.; Tseng, T. Y.; Li, M. H.; Hsu, S. T.; Lin, J. J.; Chang, T. C. Conformational Transition Of A Hairpin Structure to G-Quadruplex within the WNT1 Gene Promoter. *J. Am. Chem. Soc.* **2015**, *137*, 210-8.
48. Gray, R. D.; Trent, J. O.; Chaires, J. B. Folding and Unfolding Pathways of the Human Telomeric G-Quadruplex. *J. Mol. Biol.* **2014**, *426*, 1629-1650.
49. Mashimo, T.; Yagi, H.; Sannohe, Y.; Rajendran, A.; Sugiyama, H. Folding Pathways Of Human Telomeric Type-1 and Type-2 G-Quadruplex Structures. *J. Am. Chem. Soc.* **2010**, *132*, 14910-14918.

50. Rajendran, A.; Endo, M.; Hidaka, K.; Sugiyama, H. Direct and Single-Molecule Visualization of the Solution□State Structures of G-Hairpin and G-Triplex Intermediates. *Angew. Chem. Int. Ed.* **2014**, *53*, 4107-4112.

51. Koirala, D.; Ghimire, C.; Bohrer, C.; Sannohe, Y.; Sugiyama, H.; Mao, H. Long-Loop G-Quadruplexes Are Misfolded Population Minorities with Fast Transition Kinetics in Human Telomeric Sequences. *J. Am. Chem. Soc.* **2013**, *135*, 2235-2241.

52. Koirala, D.; Mashimo, T.; Sannohe, Y.; Yu, Z.; Mao, H.; Sugiyama, H. Intramolecular Folding in Three Tandem Guanine Repeats of Human Telomeric DNA. *Chem. Commun.* **2012**, *48*, 2006-2008.

53. Bončina, M.; Lah, J.; Prislan, I.; Vesnaver, G. Energetic Basis of Human Telomeric DNA Folding into G-Quadruplex Structures. *J. Am. Chem. Soc.* **2012**, *134*, 9657-9663.

54. Jarzynski, C. Nonequilibrium Equality for Free Energy Differences. *Phys. Rev. Lett.* **1997**, *78*, 2690-2693.

55. Mergny, J. L.; Phan, A. T.; Lacroix, L. Following G-Quartet Formation by UV-Spectroscopy. *FEBS Lett.* **1998**, *435*, 74-8.